A METHOD TO MEASURE THE PERMEABILITY OF DRY FIBER MATS

Patrik Pettersson

Research Engineer
Metso Paper Sundsvall
SE-851 94 Sundsvall, Sweden

T. Staffan Lundström

Professor
Division of Fluid Mechanics
Luleå University of Technology
SE-971 87 Luleå, Sweden

and

Tomas Wikström

PhD
Metso Paper Sundsvall
SE-851 94 Sundsvall, Sweden

(Received May 2005)

ABSTRACT

Close to the finalization of the medium density fiberboard process, a fairly thick bed of loosely entangled fibers is compressed in a belt-press to often less than a tenth of its original unstressed thickness. This single unit operation is very important to consider when the manufacturing process of the boards is to be optimized. Despite this, there is a lack of knowledge of the interaction between the fiber mat strength and how the fluid flows through it, i.e. de-aeration. Thus, it is of greatest importance to find reliable methods for studying this stage of the manufacturing process. Following this quest, a method is developed with which the gas permeability of fiber mats can be measured. The method offers the potential to measure the permeability at different flow rates and thus at arbitrary pressure gradients through the material. The method is successfully validated with a porous reference material consisting of polymer spheres, and it is shown that the flow follows Darcy's law at the flow rates of interest. Finally, the method is demonstrated by a presentation of permeability measurements on fiber mats consisting of spruce fibers.

Keywords: Medium density fiberboard, gas permeability, anisotropic permeability, experimental validation, porous flow.

INTRODUCTION

This study covers a part of the manufacturing process of medium density fiberboard, (MDF). Close to the final formation, a fairly thick mat of loosely entangled fibers is compressed in a belt-press to often less than a tenth of its original unstressed thickness. During this process, a large amount of air is forced through the porous mat generating pressure on it due to a flow resistance between the air and fibers, a procedure often termed de-aeration. The magnitude of the force is dependent on the permeability of the fiber mat, the speed of the belt, the geometry of the belt-press, and the potential for air to escape via permeable belts. If the force generated by the airflow becomes too high, the fiber mat will break. In order to mimic the flow of air and the corresponding pressure gradient, the resistance to flow must be found. One reliable method for networks with complex geometry is to measure the resistance to flow at discrete points and to fit suitable resistance models to the results. Measurements of the resistance to flow of porous materials are, however, not straightforward. To

start with, airflow through porous media does not generally follow Darcy's law. There are at least three possible reasons for this: 1) The Reynolds number, in many cases, becomes too high and inertia effects must be considered. Inertia effect occurs when the flow regime is approaching the transition region between laminar and turbulent flow. The inertia effect is usually dealt with by using the Forchheimers Equation (Whitaker 1996) that may be written as follows:

$$-\frac{\partial p}{\partial x} = \frac{\mu}{k} v + \beta \rho_g v^2 , \qquad (1)$$

where p is the pressure, v the superficial velocity, μ the viscosity, k and β parameters of the porous media, and ρ_g the fluid density. If β is set equal at zero, k becomes equal to the permeability K and the Darcy's equation is found. Hence, in order to use Eq. (1), two material parameters must be determined. 2) Besides inertia effects, if the pressure drop caused by the flow rate overcomes the fiber mat stress, the fiber mat may deform. This phenomenon has been shown to result in a linear pressure velocity relationship up to a certain pressure difference, while above this pressure the velocity remains constant as the driving pressure is increased (Belkacemi and Broadbent 1999). 3) The non-Darcian behavior can also be attributed to the molecular effect being important for gas flow at low pressures in very small pores. The effect is that measured gas permeability is higher than liquid permeability in the same porous media (Bear 1972; Scheidegger 1972). The reason for this is that the mean free path of the gas molecules approaches the dimensions of the pores. This results in a Knudsen flow, implying that there is a slip between the walls of the pores and the gas. That would result in a too high measured flow rate for a given pressure drop. For N_2 at a pressure of one atmosphere and a temperature of 300 K, the mean free path is 22 nm (Thompson 1972).

There are a substantial number of published findings on the permeability of liquids penetrating fiber networks, while only a few studies consider characteristics of the flow of gas through fiber networks. One technique often used with liquids that also applies to gases is the parallel flow saturated technique, which is very simple and has also proven to be reliable, (Lundström et al. 2000). One drawback that must be kept in mind, however, is that relatively large channels may be formed between the sealing and the fiber mat leading to too high flow rates and incorrect permeability values. Another disadvantage is that errors in permeability values are obtained if the flow is not in the main permeability directions (Lundström et al. 1998). Only a few studies are available regarding gas flow. Sullivan and Hertel (1940) estimate the permeability of glass fibers, while Bouazza and Vangpaisal (2003) focus on clays. In both cases, the measurement is carried out in a fixed control volume where the pressure drop is carefully measured at a constant flow rate. Yet another approach for determining permeability and often applied to fibrous material is to use dynamic compression equipment. A permeability model has been established for pulp at low basis weight for this type of set-up (Buntain and Bickerton 2003). One uncertainty in this kind of experiment is that the volume fraction in the suspension is not generally constant in the compression direction (Zhu et al. 1995; Lu et al. 1998).

The objective of this paper is to present an evaluation of equipment that has been developed to measure the gas permeability of a porous material consisting of wood fibers, typically a fiber mat. The equipment offers the potential to measure the permeability in two independent directions in order to classify the degree of anisotropy at different flow rates and different pressure gradients.

MATERIALS

Permeability measurements were carried out on two types of material: reference material expandable polystyrene (EPS) spheres used to validate the permeability equipment, and fiber mats, which are the main constituents in the MDF material. The EPS material has the following advantages when using it as a reference material: 1) Its permeability is in the same range as the fiber network at high porosity; 2) It is stable

under testing conditions; 3) Its permeability can be estimated by analysis. To fulfill these requirements, EPS spheres with a mean diameter of 0.62 mm, delivered by the Finnish company StyroChem, were used. This polymer is made of styrene containing pentane as a blowing agent. An image analysis of the spheres was performed in order to estimate their diameter. The image analysis was conducted by examining the spheres in a microscope connected to the software "Image pro plus." The analyzed image had a resolution of about 47 pixels per mm, depicted in Fig. 1. The categorization of single spheres was accomplished by setting a threshold value for the roundness defined as:

$$r = \frac{S_s^2}{4 \cdot \pi \cdot A_s}. \tag{2}$$

Here S_s describes the perimeter and A_s denotes the cross-sectional area of the spheres, respectively. Hence, for a perfect spherical particle, the roundness value is 1.0. The area in Fig. 1 that deviates from spherical shape was excluded in the analysis of the diameter of the spheres by setting the roundness value at 1.1. By varying the roundness value from 1.1 to 1.5, the mean diameter changed by only 0.8%. Several methods were tested to determine the porosity of the EPS spheres under dry conditions. The porosity of a material is defined as the fraction of the bulk volume of the porous sample that is occupied by pore or void space. The methods used when estimating the porosity of the EPS material were based on the density method, which yields the total porosity. The density method depends on the ratio between the bulk density of the sample and the density of the solid particles. The density of the EPS spheres, ρ_s, was obtained from the supplier, 1010 kg/m^3; the bulk density, ρ_c, was determined by measuring the mass of the spheres used in the measurement, (cf. Fig. 2). The total porosity is expressed as:

$$\varepsilon_s = 1 - \frac{\rho_c}{\rho_s}. \tag{3}$$

Spruce chips from Östrand, Sweden, were degenerated in a burnisher equipment at the Technology Center in Sundsvall, Sweden. The outcome from the equipment is fibers. Of importance, the fibers are relatively long and strongly

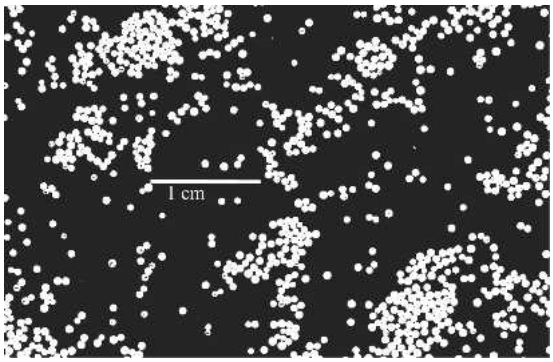

FIG. 1. A part of the image used in the image analysis of the spheres. The length scale is 10 mm. The areas that consist of too densly packed spheres deviate from a spherical shape and are excluded from the analysis by setting the roundness value at 1.1.

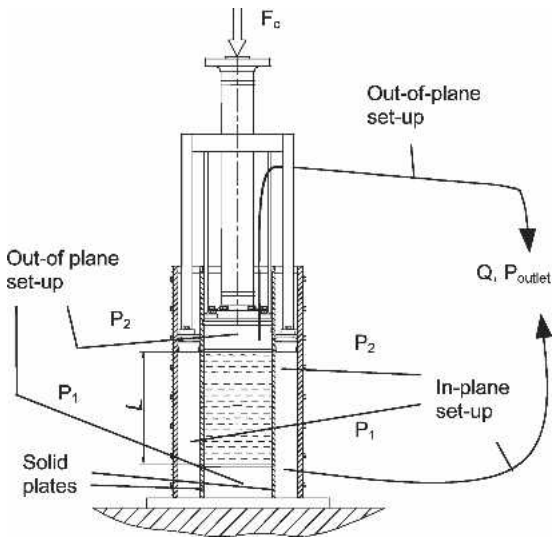

FIG. 2. Schematic sketches of the measuring cell for set-up. Index 1 and 2 denote the inlet and outlet, respectively. The pressure transducers located as illustrated in the sketch measure the pressure drop of the gas through the porous material. During the measurement, air is transported in a tube out from the equipment where the flow rate and air pressure are measured in order to determine the mass flow. For the in-plane set-up, a pair of rubber cloths was placed in the top and bottom position of the porous material. In that set-up, the solid plates were exchanged to perforated plates with holes of a diameter of 1 mm.

crimped, thus enabling entanglement to neighboring fibers as illustrated in Fig. 3. In order to determine the geometrical parameters of the fibers forming the networks, an image processing was performed by using Pulp Quality Monitor (PQM)™ equipment. This system gives the fiber diameter as an arithmetic mean value, while the fiber length is specified as a weighted average length. The coarseness value is calculated from the total measured fiber length and the mass of the fiber sample. The resolution of the image obtained was about 15 μm per pixel. The morphological data of the measured spruce fibers are depicted in Table 1. The results from the refining illustrate that the outer mean diameter of the fibers is in the same range, except for the fibers that were degenerated one year later.

As for the bed of spheres, it is important to determine the porosity of the fiber mat. This is not straightforward since the fibers themselves are porous, (cf. Fig. 4), i.e. a wood chip consists of many hollow fibers. Hence, a number of correlation parameters have been presented for pulp suspension; one important parameter is the total porosity described by Wikström and Rasmuson 1998 and Vomhoff and Norman 2001. The total porosity is defined as the total volume of voids, i.e. both lumen volume and the free pore space outside the fibers in relation to the total control volume, illustrated by Wikström and Rasmuson (1998), compare Fig. 5, which may be expressed as:

$$\varepsilon_t = 1 - \frac{V_f}{V_f + V_{lu} + V_g}, \qquad (4)$$

where ε_t describes the total porosity for the fiber mat, the fiber wall volume V_f, the free volume between the fibers V_g, and the lumen volume inside the fibers V_{lu}. The total porosity for the fiber mats can also be expressed in terms of the

FIG. 3. A typical high porosity fiber mat with fibers that are loosely entangled to each other. Length scale indicates mm.

TABLE 1. *The morphological data of the spruce fiber mats and the dryness value of the material at the time of the measurements. Batch 4 denotes the measurement conducted more than one year later compared to the other ones.*

Batch no.	Average outer diameter [μm]	Average fiber length [mm]	Coarseness value [mg/m]	Dryness [kg/kg]
1	29.0	1.80	0.50	0.93
2	29.3	1.84	0.43	0.93
3	28.5	1.85	0.37	0.93
4	32.18	2.14	0.64	0.91

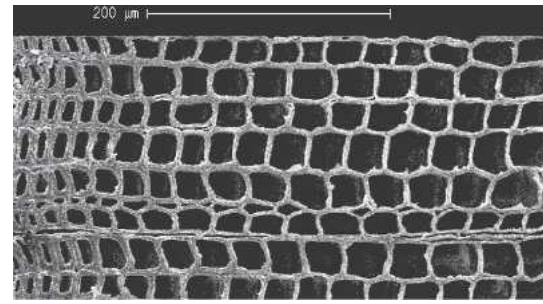

FIG. 4. Schematic picture of the internal structure of a cross-section of a wood chip displaying the fiber geometry, (with permission from Staffan Palovaara, SCA Research). The fibers are separated from each other in the burnisher equipment.

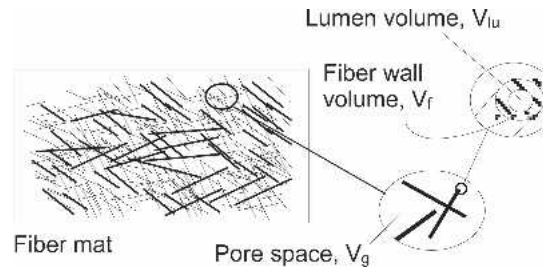

FIG. 5. Definition of the different volumes in a fiber mat.

density method suggested by (Vomhoff and Norman 2001) as:

$$\varepsilon_t = 1 - \frac{w}{h \cdot \rho_f}, \tag{5}$$

where w is the basis weight, h the thickness of the sample, and ρ_f the fiber wall density.

MEASURING UNIT

To experimentally derive the permeability of the fiber mats, a permeability measurement unit has been developed which is designed for measurements of in-plane permeability as well as out-of-plane permeability, (Fig. 2). If the latter direction coincides with one principal direction, the full 3D-permeability tensor can be derived. To determine the permeability for the porous material, Darcýs law is used:

$$\frac{\partial p}{\partial x} = -\frac{\mu}{k} v, \tag{6}$$

where v is the superficial velocity, μ is the dynamic viscosity of the fluid, K represents the intrinsic permeability, and the gradient on the left-hand side is the pressure drop of the fluid. Since air is a compressible fluid, it is necessary to rewrite Darcýs law by use of the equation of state:

$$pvA_c = \dot{m}RT, \tag{7}$$

where R is the gas constant, T is the temperature of the gas, p is the fluid pressure, A_c is the cross-sectional area of the cavity, and $\dot{m}$ the mass flow. By integrating the combination of Darcy's law (Eq. 6) and the equation of state for air (Eq. 7) in the flow direction and by assuming a homogenous porosity profile, the gas permeability is expressed as:

$$K = \frac{2\mu\dot{m}RTh}{A_i(p_1^2 - p_2^2)}. \tag{8}$$

To derive the out-of-plane permeability, air is forced through a perforated plate placed at the base of the measuring cell and into the fiber network by the means of an applied pressure gradient, (cf. Fig. 2). The air is allowed to leave the cell through a perforated top wall. Maximum volume of the cavity is 0.19 m × 0.311 m × 0.4 m where the last dimension denotes the height. In the current set-up, flowmeters (4 to 25 m^3/h, or 30 to 390 m^3/h) were connected externally with the permeability equipment at the outlet by a tube with an accuracy of ±0.5% of the calibrated span. In addition, a pressure transducer ranging from 0 to 16 kPa was placed close to the flow gauges in order to determine the mass flow. Pressure transducers (0 to 20 kPa, or 0 to 200 kPa) were also connected to the permeability equipment at the inlet position, marked as p_1 in Fig. 2; the sensitive one was used when possible in order to reduce experimental error. The pressure transducer placed at the outlet had a range of 0 to 7.5 kPa, marked as p_2 in Fig. 2. The measurement error of the pressure transducers was ±0.2% of the calibrated span. The height was measured by a linear magnetic position sensor with a measuring length of 1.0 m. The maximum deviation of the magnetic position sensor was ± 0.05% of the calibrated span. The permeability measurements were conducted under stationary conditions in the sense that a constant flow rate was applied through the fiber mat while the height of the cavity was held constant. Since the permeability of the fiber mat is strongly dependent on the porosity, additional measurements were performed by lowering the upper plate. This procedure was repeated until the lowest possible volume of the cavity was reached, with respect to the limit of the pressure transducer, or until the maximum load from the compression was achieved.

For the measurement of the in-plane permeability, the solid walls were replaced with perforated plates, and rubber cloths were placed on the top and bottom surfaces to prevent air from leaving the cavity in the out-of-plane direction. Air was forced through the sample from the left chamber to the corresponding right one, cf. (Fig. 2) where the positions of the pressure transducers can be spotted.

The systems presented have several sources of error such as:

- Pressure losses through the sealing between the piston and solid walls,
- Edge effects in the fiber mat closest to the solid wall,
- Pressure, flow rate, and position transducers,
- Non-uniform flow rate due to compression of air,
- Temperature variations inside the cavity due to variation in temperature of the flowing gas.

Some of the sources are more difficult to estimate than others, but by studying their effects on the permeability in Eq. (8), it is possible to distinguish the most sensitive ones. By scrutinizing the parameters, it is obvious that the inlet and outlet pressure must be measured very accurately. In addition to this, a pressure loss test without fibers in the cavity was performed in order to study how the flow resistance through the perforated walls influenced the permeability. It was shown that the pressure drop through the walls was negligible.

A final remark on the performance of the measurement is that a fiber bed with no constraints would compress homogeneously. A hypothesis is that with constraints, for instance due to friction at the side walls, an inhomogeneous material may be obtained, the estimation of the permeability due to that effect will be misleading. Hence, during the permeability measurements, the applied force on the fiber bed was logged showing that the reaction force from the bed towards the piston decreased during the measurement, i.e. the fibers were redistributed. The permeability measurement was not established until force equilibrium was reached.

RESULTS AND DISCUSSION

Validation of permeability equipment

Measurements carried out in the out-of-plane set-up show that the apparent permeability of the EPS spheres is dependent on the Reynolds number defined as:

$$\mathrm{Re} = \frac{v \cdot d \cdot \rho_g}{\mu}, \qquad (9)$$

where v is the superficial velocity, i.e. flow rate divided by the cross-sectional area of the cavity, d is a characteristic length scale, which for the spheres was set at the average mean diameter, (cf. Fig. 6). At high Reynolds number, the reduction in apparent permeability is in accordance with the classic results obtained by Rumpf and Gupte (1971), who attribute these phenomena to inertial effects, (cf. Eq. 1). At low Reynolds number, the strong non-Darcian behavior can either be due to the Knudsen effect discussed in the introduction or may just be a result of erroneous values obtained from the measurement sensors. The latter is a result of low flow rates and a correspondingly low pressure drop that was generated. One consequence of a Knudsen flow is that the quantity of gas flowing through a capillary is larger than would be expected from the Poiseuille's formula at low pressure-driven flows. This occurs in cases where the distance between the walls inside the porous material is in the same magnitude as the free molecular path length of the flowing fluid. The Darcy's law applies for Reynolds numbers approximately between 3 and 12, (cf. Dullien 1992). By performing measurements in this

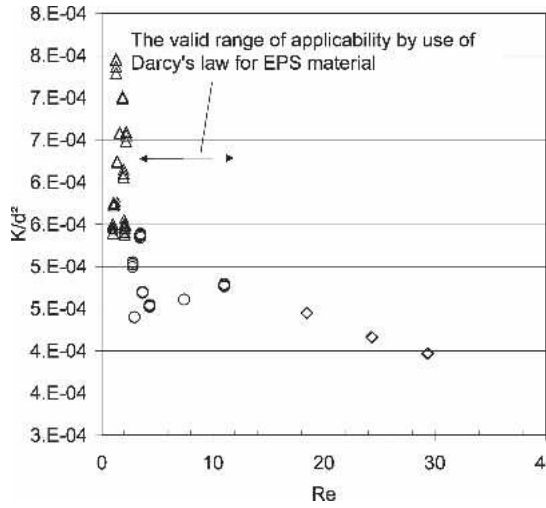

FIG. 6. Non-dimensional apparent permeability of the EPS material. Triangles illustrate the permeability measurements conducted at too low Reynolds numbers. The valid range of applicability of Darcy's law is marked as circles. The diamonds denote a too high flow rate where the inertia effects occur, cf (Dullien 1992).

range, the equipment can be validated by comparing results to theoretically derived expressions for permeability. One such expression that has been successfully validated with experiments is the one derived by Rumpf and Gupte (1971):

$$K = \frac{d^2 \cdot \varepsilon_s^{5.5}}{5.6 \cdot S}, \qquad (10)$$

where d is the diameter of the spheres, ε_s is the porosity of the spheres, and S is a shape factor equal to one for a narrow distribution of diameters and equal to 1.05 for wider ones. Setting S at 1.0, being the most appropriate presumption for the bed of spheres, yields a fit to the measured permeability, (cf. Fig. 7).

Permeability of fiber mats

In order to evaluate the equipment for fiber mats, the permeability was measured as a function of time and Reynolds number. Regarding the function of time, the permeability was practically the same when the measurements were carried out with more than one year's interval on two different batches. The batches were formed and degenerated at the specific day when the measurements were conducted, (cf. Fig. 8 and Table 1). This indicates that the permeability equipment is stable, and the procedure of forming the fiber mat has been similarly performed, i.e. the systematical errors have the same influence on the permeability measurements on the different fiber mats. A direct comparison between the permeability measurements gives a maximum deviation of less than 8%. Unlike the permeability measurement on spheres, the permeability on fiber mats was unaffected by the Reynolds number in the measured flow interval, (Fig. 9), i.e. Darcy's law is due to that valid. The Reynolds number for the gas flowing through the fiber mat was defined in a similar procedure as for the EPS material, (cf. Eq. 9). The characteristic length scale was set at the average fiber diameter obtained from the PQM measurement.

Results of the measured permeability for the fiber mat in the in-plane and in the out-of-plane direction are given in Fig. 10. It is shown that the permeability of the spruce fiber mats has an anisotropic behavior at low porosity as outlined by Håkanson et al. (2005) for similar material. In

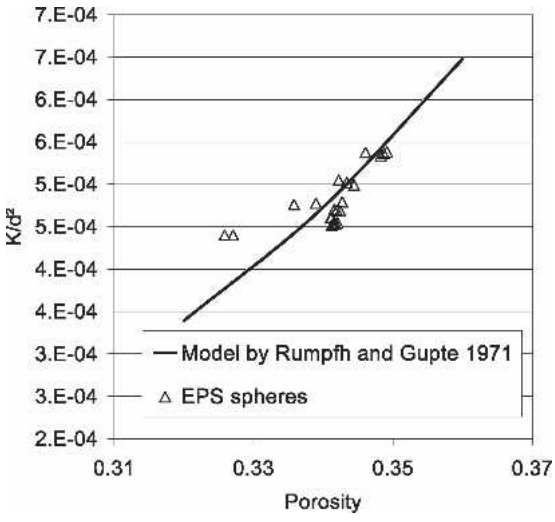

FIG. 7. Comparison between measured permeability values of bed of EPS spheres and a theoretical model proposed by Rumpf and Gupte (1971), Eq. (10).

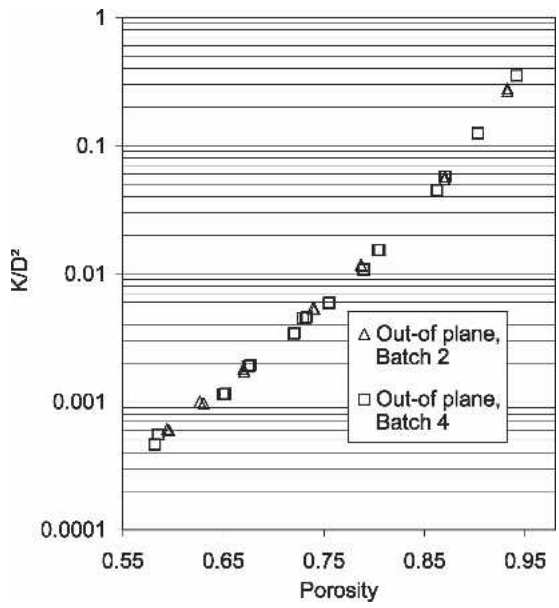

FIG. 8. Comparison between measured non-dimensional permeability of spruce fiber mats generated at different moments. The materials were degenerated and formed at the time just before each of the measurements.

TABLE 2. *The empirical constants for the permeability model valid for the fiber mats depicted in Fig. 10 and the R^2 value of the fitted modes.*

Permeability model	C_1	C_2	C_3	R^2
Spruce fiber; out-of-plane direction	0.148	8.168	1.691	0.948
Spruce fiber in-plane direction	0.414	15.259	0.981	0.979

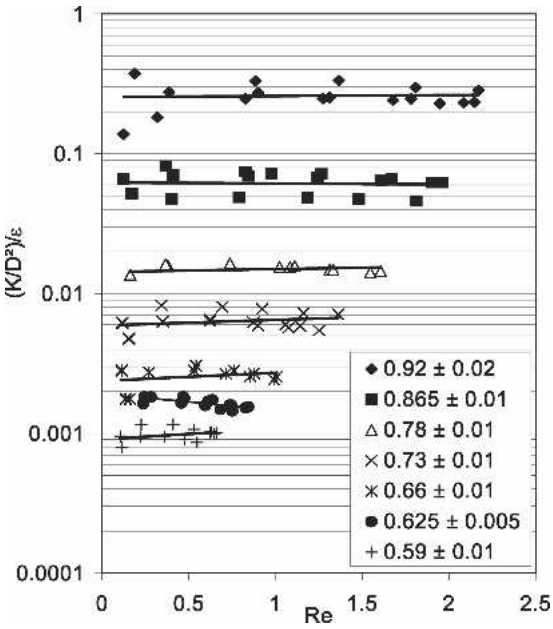

FIG. 9. Non-dimensional permeability for the measured fiber mats divided by the porosity. A least square fit of the plotted data illustrates the trend of each group respectively. The experimental data were collected in groups of different values of porosity where the deviation in each group is illustrated in the legend. The graph shows that the permeability for the fiber mat is independent of the flow rate in the measured range, i.e. no inertia effects.

order to find the level of anisotropy, the measured permeability was fitted to the following empirical equation, similar to the equation found by Koponen (1998) for pulp suspensions:

$$k = D^2 \cdot \frac{C_1}{(e^{(C_2 \cdot (1-\varepsilon_t))} - 1)^{C_3}}, \qquad (11)$$

where C_1, C_2 and C_3 are empirical constants for the wood fiber mats, (cf. Table 1), ε_t is the total porosity of the fiber mat, and D is the diameter of the fiber. The percentage difference between the in-plane and out-of-plane permeability is illustrated in the right-hand axis in Fig. 10. The measurement at high porosity should give the same permeability since the fiber mat is formed in a procedure where the fibers are more or less randomized. Even though the forming of the fiber mat was performed in a similar procedure, an oriented fiber mat could have occurred, since the first permeability value was determined at a lower porosity level than the actual forming one. At lower porosity, the difference between the in-plane and out-of-plane direction is around 40%. A re-arranged fiber mat from a random to an oriented structure could explain the differences in the results. If so, the differences should go towards an asymptotic relationship since the permeability is solely dependent on the geometry of the material (Scheidegger 1972). The geometrical dependency of the permeability is related to the square of a typical length scale such as the particle diameter. If the material is rearranged from a randomized to an orientated fiber mat structure, the typical length scale in the flow direction would change. Consequently, the ratio of the permeability in out-of plane and in-plane direction would go towards an asymptotic value.

CONCLUSIONS

A method has been developed with which the gas permeability of fiber mats can be measured. The equipment was successfully validated with a porous bed consisting of polymer spheres following the results given by Rumpf and Gupte (1971). With the spheres, it was shown that the flow follows Darcy's law in an intermediate range of Reynolds numbers approximately between 3 and 12. At higher Reynolds numbers, the apparent permeability decreased, which can be related to inertia effects. At lower Reynolds numbers, the increased permeability can be explained by the Knudsen effect, as pointed out by Bear (1972) and Scheidegger (1972) or by experimental errors.

None of these phenomena were observed in

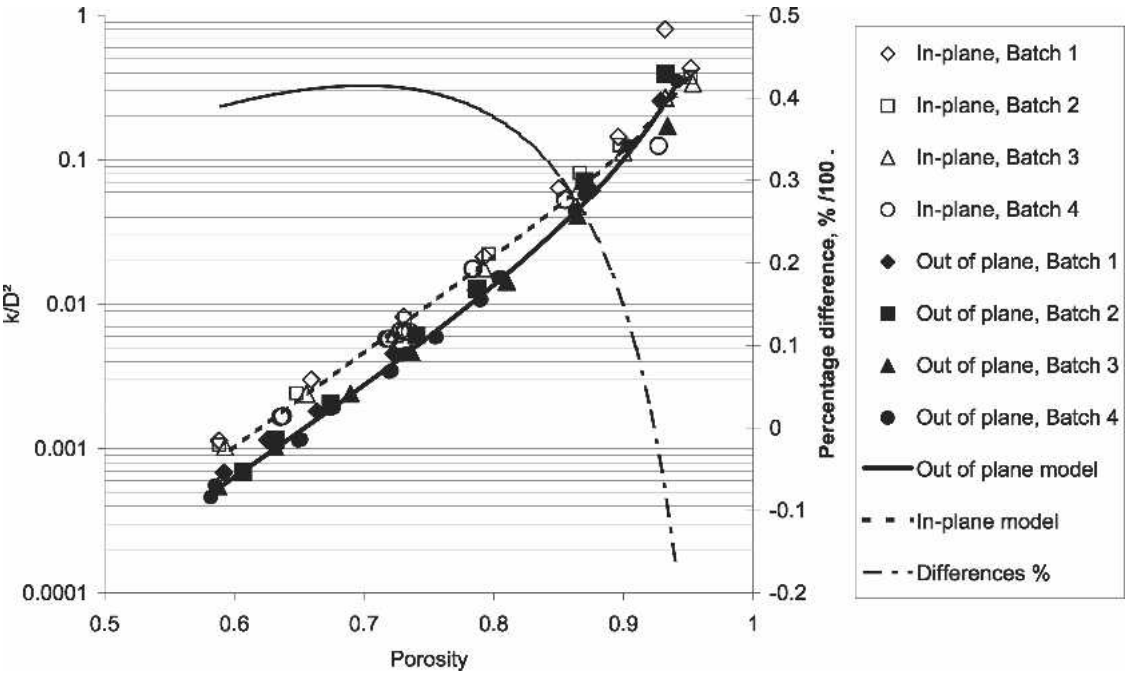

FIG. 10. Non-dimensional plot of measured permeability on spruce fiber mats. Data points are from measurement performed in in-plane and out-of-plane direction. The permeability model described in Eq. (11) has been used to determine the percentage difference between the out-of-plane and in-plane differences. The empirical constants are given in Table 2.

the fiber mat measurements. Regardless of the fiber volume fraction, the permeability was not influenced by Reynolds number at the condition tested. The level of the measured fiber mat permeability was about three levels of magnitude lower to two times higher than the measured permeability of the bed of spheres.

As final quality control of the method, the permeability of fiber mat produced in the same burnisher equipment was measured but separated by an interval of more than one year. The permeability of these fiber mats had practically the same permeability versus porosity relationship. This finding really ensures us that the method has been valid for all experimental series.

The permeability experiments for the in-plane and out-of plane direction indicated that the distribution of fibers at high porosity is oriented more or less randomly. A hypothesis is that the compression of the fiber mat forces the fibers to re-arrange from a random to an oriented structure. The structural changes inside the fiber mat result in a network with an anisotropic behavior, which seems to be the case in the low porosity region. Such behavior is outlined elsewhere (Håkanson et al. 2005) for a similar material.

In summary, the method developed is reliable and seems to produce results with high quality. This encouraged us to expand the experimental study and deepen the analysis in order to present a model of the de-aeration of the belt-press in a forthcoming paper.

NOMENCLATURE

A = The cross-sectional area [m^2]
C_1, C_2, C_3 = Empirical constants for the permeability model valid for fiber mats
D = Fiber diameter [m]
d = Sphere diameter [m]
F = Applied force [N]
h = Sample thickness [m]
K = Intrinsic permeability [m^2]
k = Parameter in Forchheimers formulation [m^2]

$\dot{m}$ = Mass flow of the fluid [kg/s]
p = Air pressure [Pa]
R = Gas constant (air as an ideal gas R = 287 at T = 300 K) [J/kg K]
r = Roundness value of the spheres
S = Shape factor
T = Temperature of the gas [K]
V = Volume [m^3]
w = Basis weight of fiber sample [kg/m^2]
x = Measurement direction in the permeability equipment [m]

Greek

β = Parameter in Forchheimers formulation [1/m]
ε = Total porosity of the measured material
μ = Dynamic viscosity [Pas]
ρ = Density of the specific material [kg/m^3]
ρ_b, = Bulk density of fiber mat [kg/m^3]
ρ_c = Bulk density of spheres [kg/m^3]
v = Superficial fluid velocity [m/s]

Index

$_c$ = cavity
$_f$ = solid, i.e. fiber wall
$_g$ = air
$_{lu}$ = lumen
$_s$ = spheres
t = fiber mat

REFERENCES

BEAR, J. 1972. *Dynamics of fluids in porous media*. American Elsevier, New York, NY.

BELKACEMI, K., AND A. D. BROADBENT. 1999. Air flow through textiles at high differential pressures. Textile Res. J. 69(1):52–58.

BOUAZZA, A., AND T. VANGPAISAL. 2003. An apparatus to measure gas permeability of geosynthetic clay liners. Geotextiles and Geomembranes 21:85–101.

BUNTAIN, M. J., AND S. BICKERTON. 2003. Compression flow permeability measurement: A continuous technique, Elsevier Science Composite, Auckland, New Zealand. Part A 34:445–457.

DULLIEN, F. A. L. 1992. Porous media: Fluid transport and pore structure, Academic Press, San Diego, CA.

HÅKANSON, J. M., S. TOLL, AND T. S. LUNDSTRÖM. 2005. Liquid permeability of anisotropic fibre webs. Textile Res. J. 75(4):304–311.

KOPONEN, A. 1998. Simulations of fluid flow in porous media by lattice-gas and lattice-boltzman method. Research Report 5. Department of Physics, University of Jyväskylä, Finland.

LU, W. M., Y. P. HUANG, AND K. J. HWANG. 1998. Methods to determine the relationship between cake properties and solid compressive pressure. Tamsui. Elsevier. Separation and Purification Technol. 13 1998:9–23.

LUNDSTRÖM, T. S., B. R. GEBART, AND E. SANDLUND. 1999. In-plane permeability measurements on fibre reinforcements by the multi-cavity parallel flow technique. Polymer Composites 20:146–154.

———, R. STENBERG, R. BERGSTRÖM, H. PARTANEN, AND P. A. BIRKELAND. 2000. In-plane permeability measurements: A Nordic round-robin study. Composites: Part A 31:29–43.

RUMPF, H., AND A. R. GUPTE. 1971. Chem. Ing. Tech. 43(6):367–375.

SCHEIDEGGER, A. E. 1972. The physics of flow through porous media, University of Toronto Press, Toronto, Canada.

SULLIVAN, R. R., AND K. L. HERTEL. 1940. The flow of air through porous media, J. Appl. Physics 11:761–765.

THOMPSON, P. A. 1972. Compressible-fluid dynamics. Mcgraw-Hill Book Company, New York, NY.

VOMHOFF, H., AND B. NORMAN. 2001. Method for the investigation of the dynamic compressibility of wet fibre networks. Nordic Pulp Paper Res. J. 16(1):57–62.

WIKSTRÖM, T., AND A. RASMUSON. 1998. Yield stress of pulp suspensions. Nordic Pulp Paper Res. J. 13:243–250.

WHITAKER, S. 1996. The Forchheimer Equation: A theoretical development. Transport in Porous Media 25:27–61.

ZHU, S., H. R. PELTON, AND K. COLLVER. 1995. Mechanistic modelling of fluid permeation through compressible fiber beds. Chemical Eng. Sci. 50(22):3557–3572.